depending on the identity of the initial and final states involved in the mixing. These cross sections are large enough for a mixing collision to occur at 10 Torr or less, depending on the transition, on a 10-ns time scale. The two transitions where we observe the most obvious deviation from Townsend behavior both involve the $3d^4 4s(a^6D)4p\ ^7P^0$ excited state. Changing the alignment of the molecular/atomic transition dipole relative to the radiation field polarization axis could affect the net rate of multiphoton absorption, leading to deviations from Townsend behavior. It is also possible that field-induced dipole moments could change the cross sections. This would be consistent with the enhanced deviations at higher plate voltages. This type of effect could be isolated by measuring the MPI polarization ratio[16,17] dependence on pressure.

One final set of collisional effects which may affect ion yields in a pressure-dependent manner are those involving collisions between excited-state buffer gas atoms themselves or ionization caused by photons emitted by these excited atoms. These excited-state atoms could be created by electron impact or by vacuum-UV absorption. There are a number of secondary channels for ionization which make Townsend theory analysis difficult at higher pressures. A closely related area, optical pumping and collisional energy transfer leading to emission in laser-induced plasmas, is the subject of a great deal of research due to the possibility of producing short-wavelength population inversions in these systems.[34] The wavelength resolution and pressure dependence of the coherent laser-induced emission and the fluorescence 90° to the laser, along with obtaining mass-resolved ion yields, should aid in determining the extent of the contribution to the ion signal by processes involving excited-state buffer gas atoms.

(34) Harris, S. E., Lucatorto, T. B., Eds. *Laser Techniques in the Extreme Ultraviolet*; American Institute of Physics: New York, 1984.

Conclusions

Simple ion multiplication theory is the appropriate starting point for analysis of the pressure dependence of MPI signals in bulk gas experiments. The multiplication theory must hold in order for the measured ion signal to accurately reflect the initial MPI yield. In our experiments we have found that Townsend ion multiplication theory fits most of our data for MPI signals of ACTs in the presence of helium and argon. In the region where we do product-state analysis, multiplication is clearly the dominant means of ion production. In this case, intermolecular relaxation effects are negligible on the time scale of the laser pulse. In some other cases there is the need for further experiments to determine the exact nature of the predominate mechanism of ion production. Frequency up-conversion, collisionally induced intramultiplet mixing, and other ionization processes involving excited-state buffer gas atoms are possible causes of the deviations from Townsend theory behavior. Work is in progress to identify and quantify the secondary effects leading to these deviations. The experimental results presented here demonstrate the necessity of examining the pressure effects in any bulk gas MPI system where branching ratios are determined based on relative intensities. For species with much higher vapor pressures, such as $Cr(CO)_6$, the possibility of self-multiplication must be included in the analysis of MPI signal pressure dependence. Bulk gas MPI experiments performed in the absence of buffer gas should therefore also be examined for deviations from multiplication behavior before the relative intensities of spectral features are analyzed.

Registry No. $Cr(CO)_6$, 13007-92-6; He, 7440-59-7; Ar, 7440-37-1; Xe, 7440-63-3; ethylbenzene $Cr(CO)_3$, 12203-31-5.

Energy Dependence of Collisional Deactivation of Highly Vibrationally Excited Ethylcycloheptatriene

Gui-Yung Chung and Robert W. Carr*

Department of Chemical Engineering and Materials Science, University of Minnesota, Minneapolis, Minnesota 55455 *(Received: October 14, 1986; In Final Form: December 29, 1986)*

Collisional self-deactivation of 7-ethylcycloheptatriene photoactivated to total internal energies of 123 kcal/mol (240 nm), 111 kcal/mol (265 nm), 106 kcal/mol (280 nm), and 100 kcal/mol (295 nm) has been investigated. The reaction products consisted of the positional isomers 1-, 2-, and 3-ethylcycloheptatriene and methyl-ethyl-substituted benzenes formed by structural isomerization. The pressure dependence of reaction products resulting from positional and structural isomerization was determined at each wavelength in a series of experiments without added bath gases. The yield of structural isomerization products decreased with increasing pressure, indicative of collisional stabilization of photoactivated ethylcycloheptatrienes. The ratio of positional to structural isomerization products increased with increasing pressure at fixed wavelength and increased with increasing wavelength at fixed pressure, consistent with a shorter lifetime for positional isomerization than for structural isomerization. Master equation calculations were done using RRKM theory and a stepladder model for deactivation. The model calculations predict that the average energy removed per deactivating collision, $\langle \Delta E \rangle$, increases with increasing excess energy of photoactivated 7-ethylcycloheptatriene.

Introduction

Unimolecular reactions are controlled by competition between the rates of chemical change and intermolecular energy transfer. It has long been recognized that understanding collisional transfer of energy is a critical component in the accurate description of unimolecular reactions.

An important quantity for characterizing collisional energy transfer from highly vibrationally excited molecules is $\langle \Delta E \rangle$, the average energy transferred in all collisions. Much of the present information on $\langle \Delta E \rangle$ has been obtained from indirect experiments which require knowledge of the chemical reaction mechanism and a calibration of the deactivation rate against a strong collider or a reference unimolecular reaction. Development of experimental techniques for direct detection has permitted excited-state kinetics of highly vibrationally excited molecules to be investigated by time-resolved UV absorption spectroscopy[1] and IR fluorescence spectroscopy.[2]

Highly vibrationally excited ground-state molecules with relatively narrow energy distributions can, in favorable cases, be prepared by photoactivation. For example, excitation of 7-

(1) Hippler, H.; Luther, K.; Troe, J.; Walsh, R. *J. Chem. Phys.* **1978**, *68*, 323.

(2) Smith, G. P.; Barker, J. R. *Chem. Phys. Lett.* **1981**, *78*, 253.

0022-3654/87/2091-2831$01.50/0

ethyl-1,3,5-cycloheptatriene (7-Et-CHT) to S_1 is followed by rapid internal conversion to the ground electronic state.[3,4] The initial energy distribution in S_0* is the thermal distribution of unexcited molecules in S_0. At room temperature the average thermal energy is 3.6 kcal/mol compared with excitation energies of approximately 100 kcal/mol or more. Thus, the energy distribution of the photoactivated molecules is nearly monoenergetic.

Previous work on photoactivated 7-Et-CHT showed that values of $\langle\Delta E\rangle$ obtained by indirect experiments were significantly larger than those found by direct detection. In steady-state photoisomerization[3] $\langle\Delta E\rangle$ was obtained from Stern–Volmer plots using a collision efficiency and microcanonical rate coefficients, $k(E)$, derived from thermal isomerization experiments.[5] Direct measurement of $k(E)$ by time-resolved UV absorption after pulsed laser excitation gave a value that is 2.6 times smaller than that from RRKM fits to the thermal rate data.[4] Also, values of $\langle\Delta E\rangle$ measured directly were smaller than those obtained by analysis of steady-state data.[6] Direct and indirect measurements of $\langle\Delta E\rangle$ could be reconciled by using the direct measurement $k(E)$'s and down revision of the collision efficiency used to obtain $\langle\Delta E\rangle$ from the indirect data.[6]

The dependence of $\langle\Delta E\rangle$ on energy of the highly vibrationally excited intermediate is an important question. Barker and coworkers reported that $\langle\Delta E\rangle$ increased with increasing internal energy of photoactivated azulene in their time-resolved infrared fluorescence studies.[7,8] Dove, Hippler, and Troe[9] also found a dependence of $\langle\Delta E\rangle$ on excitation energy in their investigation of CS_2 by time-resolved hot UV absorption. On the other hand, investigations of the isomerization of toluene[10] and substituted cycloheptatrienes[6] by the UV absorption method indicated that $\langle\Delta E\rangle$ is not dependent or only slightly dependent on the excitation energy for numerous colliders. Application of the UV absorption method to azulene indicated that at vibrational energies below about 10000 cm^{-1} $\langle\Delta E\rangle$ increased with increasing internal energy, rising to a pressure-independent regime at higher energies.[11] It was argued that these results are not necessarily in conflict with those of ref 6 and 10, when experimental limits are considered.[11]

We report here the results of an indirect study of photoactivated 7-Et-CHT aimed at providing new data via an alternate experimental method, bearing on the question of the energy dependence of $\langle\Delta E\rangle$. Steady-state photolysis experiments were done at four wavelengths corresponding to excitation to energies of 100, 106, 111, and 123 kcal/mol. The absolute values of $\langle\Delta E\rangle$ were obtained by fitting the pressure dependence of reaction product yield by a master equation formulation of RRKM theory. The absolute values of $\langle\Delta E\rangle$ depend upon the microcanonical rate coefficients $k(E)$, which were adjusted to fit the experimentally measured values obtained directly by time-resolved hot absorption at 248 and 265 nm, removing the principal uncertainty of the indirect method. Furthermore, use of the master equation calculation makes it possible to obtain $\langle\Delta E\rangle$ without the need of a collision efficiency. The values of $\langle\Delta E\rangle$ obtained by incorporating a stepladder model are in excellent agreement with the value obtained by direct detection after excitation to 115 kcal/mol and, furthermore, give evidence that $\langle\Delta E\rangle$ increases with increasing energy.

Experimental Section

Steady illumination room-temperature photolyses were performed at pressures between 25 mTorr and 2 Torr of 7-Et-CHT without any bath gas at 240, 265, 280, and 295 nm. In the photolysis at 265 nm, 5 mol % of hexane was used as an internal standard. Measurements of photolysis time, relative light intensity transmitted by the reactor, and product composition were made.

7-Et-CHT was prepared by alkylation of 1,3,5-cycloheptatriene.[12-15] 7-Cycloheptatrienylium fluoroborate was prepared from 1,3,5-cycloheptatriene purchased from Aldrich Chemical Co. The salt was then allowed to react with sodium ethoxide, yielding 7-ethoxy-1,3,5-cycloheptatriene. 7-Et-CHT was obtained by reacting ethylmagnesium bromide with 7-ethoxy-1,3,5-cycloheptatriene. The 7-Et-CHT was purified by preparative gas chromatography. There was a very slow conversion to impurities, and the impurities were kept under 0.5 mol %.

An Osram HBO 500-W superpressure mercury arc lamp was the radiation source. For 265 nm, a chemical light filter, consisting of 5 cm of an aqueous 0.276 g/cm^3 $NiSO_4 \cdot 6H_2O$ solution, 5 cm of an aqueous 0.08 g/cm^3 $CoSO_4 \cdot 7H_2O$ solution, 5 cm of 1-atm Cl_2, and 1 cm of an aqueous 0.0017 g/cm^3 KI solution, was used. For other wavelengths, a Bausch and Lomb high-intensity monochromator was used. The nominal band-passes, measured with a 0.4-m Ebert mounting spectrometer, were 12.8, 10, 12.8, and 8 nm at 240, 265, 280, and 295 nm, respectively.

Gas handling was done with a conventional vacuum system having Teflon valves and an oil diffusion pump. The system was evacuated to 10^{-6} Torr before each experiment. Pressures were measured with an ion gauge and an MKS Baratron Type 222B pressure transducer. A cylindrical 55.2-cm^3 Pyrex reactor, of 10-cm length and 2.7-cm i.d., with quartz windows was used. Photolysis times varied from 0.2 to 5 h. Transmitted light was detected by a phototube and recorded on a chart recorder. The linearity of the phototube was checked with neutral density filters.

All reaction product analyses were performed on a Hewlett-Packard 5730A gas chromatograph with flame ionization detector, 3390A integrator, and gas sampling valve. Samples were taken from the reactor with the gas sampling valve after the reactor pressure was raised to 1 atm with air. A column, with GESE 52/Benton 34 (1:1) 10% on Chromosorb W-AW-DMCS 80/100, of 5-m length and 3-mm i.d., was used at 100 °C and with 30 cm^3/min helium carrier gas. The GC analysis revealed the following substances, listed here with their relative retention times, to be present: 7-Et-CHT, 1.0; 2-Et-CHT, 1.06; 3-Et-CHT, 1.18; 1-Et-CHT, 1.28; 1-methyl-4-ethylbenzene (1,4-Me-Et-Bz) and *n*-propylbenzene (*n*-Pr-Bz), 1.38; 1,3-Me-Et-Bz, 1.66; 1,2-Me-Et-Bz, 1.71. Here, 1-, 2-, and 3-Et-CHT are positional isomers and 1,2-, 1,3-, 1,4-Me-Et-Bz, and *n*-Pr-Bz are structural isomers. The positional isomers were identified by comparison with previous works,[3,16,17] and the structural isomers, with authentic samples. For positional isomers, GC sensitivities of peaks were assumed to be the same. In addition, small amounts (<1%) of lower molecular weight species were found but not identified.

Results

Mechanism. The reaction paths for the positional and structural isomerization of 7-Et-CHT are considered to be analogous to those of 7-methyl-1,3,5-cycloheptatriene (7-Me-CHT). The mechanism, shown in reaction a and Figure 1, is consistent with the experimental results. A dagger denotes an electronically excited

$$\text{7-Et-CHT} \xrightarrow{h\nu} \text{7-Et-CHT}^{\dagger} \rightarrow \text{7-Et-CHT*} \qquad \text{(a)}$$

molecule, and an asterisk designates a vibrationally excited molecule. 7-, 3-, 1-, and 2-Et-CHT are positional isomers. The structural isomers consist of *n*-Pr-Bz, 1,2-Me-Et-Bz, 1,3-Me-Et-Bz, and 1,4-Me-Et-Bz. These products were also reported by Troe and Wieters.[3]

(3) Troe, J.; Wieters, W. *J. Chem. Phys.* **1979**, *71*(10), 3931.
(4) Hippler, H.; Luther, K.; Troe, J.; Wendelken, H. J. *J. Chem. Phys.* **1983**, *79*, 239.
(5) Asholz, D. C.; Troe, J.; Wieters, W. *J. Chem. Phys.* **1979**, *70*, 5107.
(6) Hippler, H.; Troe, J.; Wendelken, H. J. *J. Chem. Phys.* **1983**, *78*, 6718.
(7) Rossi, M. J.; Barker, J. R. *Chem. Phys. Lett.* **1982**, *85*, 21.
(8) Rossi, M. J.; Pladziewicz, J. R.; Barker, J. R. *J. Chem. Phys.* **1983**, *78*, 6695.
(9) Dove, J. E.; Hippler, H.; Troe, J. *J. Chem. Phys.* **1985**, *82*, 1907.
(10) Hippler, H.; Troe, J.; Wendelken, H. J. *J. Chem. Phys.* **1983**, *78*, 6709.
(11) Hippler, H. *Ber. Bunsenges. Phys. Chem.* **1985**, *89*, 303.
(12) Frankel, G.; Garter, R. E.; McLachlan, A.; Richards, J. H. *J. Am. Chem. Soc.* **1960**, *82*, 5846.
(13) Conrow, K. In *Organic Synthesis*; McKusick, B. C., Ed.; Wiley: New York, 1963; Vol. 43, p 101.
(14) Conrow, K. *J. Am. Chem. Soc.* **1961**, *83*, 2343.
(15) Harrison, A. G.; Honnen, L. R.; Dauben, H. J.; Lossing, F. P. *J. Am. Chem. Soc.* **1960**, *82*, 5593.
(16) Egger, K. W. *J. Am. Chem. Soc.* **1967**, *89*(15), 3688.
(17) Egger, K. W. *J. Am. Chem. Soc.* **1968**, *90*(1), 6.

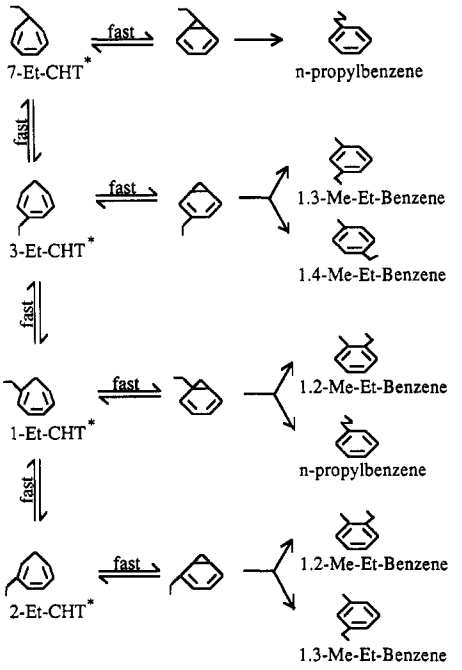

Figure 1. Isomerization processes in the steady-state photolysis of 7-Et-CHT. Vertical direction is the positional isomerization by 1,5-hydrogen transfer, and horizontal direction is the structural isomerization via ethylbicyclohepta-2,4-diene intermediate.

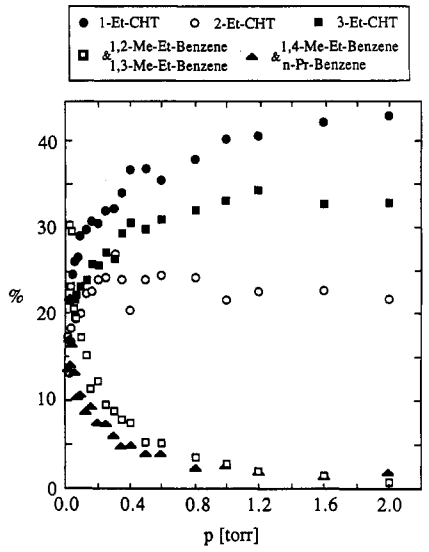

Figure 2. Change of percentages of products with pressure at 265 nm.

The light absorption is followed by a fast internal conversion to vibrationally highly excited electronic ground-state molecules. Then, positional isomerization and structural isomerization occur. Positional isomerization occurs via consecutive 1,5-hydrogen-transfer reactions with an activation energy of about 32 kcal/mol.[16] Rate constants for positional isomerization are considerably larger than those for structural isomerization, and it is understood that positional isomerization occurs before structural isomerization and governs the distribution of various structural isomerization products.[18] The yields of the collisionally stabilized 7-, 3-, 1-, and 2-Et-CHT isomers are expected to be proportional to the relative contributions to the total vibrational densities of states at the excitation energy.[3]

The pressure dependence of products formed at 265 nm are shown in Figure 2. The yield of structural isomers decreases with increasing pressure, consistent with collisional stabilization of hot 7-Et-CHT. The yield of positional isomers, on the other hand, increases with increasing pressure to a high-pressure asymptote.

(18) Egger, K. W. *J. Am. Chem. Soc.* **1968**, *90*(1), 1.

TABLE I: Composition Change with Wavelength of Light in the Steady-State Photolysis of 7-Et-CHT at 100 mTorr

	yields, %			
products	240 nm (300 min)	265 nm (5 min)	280 nm (120 min)	295 nm (260 min)
7-Et-CHT	93.06	94.64	94.41	95.17
1-Et-CHT	1.23	1.89	1.51	1.94
2-Et-CHT	1.03	0.93	1.71	1.17
3-Et-CHT	0.88	1.22	1.8	1.58
1,2-Me-Et-Bz, 1,3-Me-Et-Bz	2.5	0.77	0.3	0.14
1,4-Me-Et-Bz, *n*-Pr-Bz	1.3	0.54	0.27	

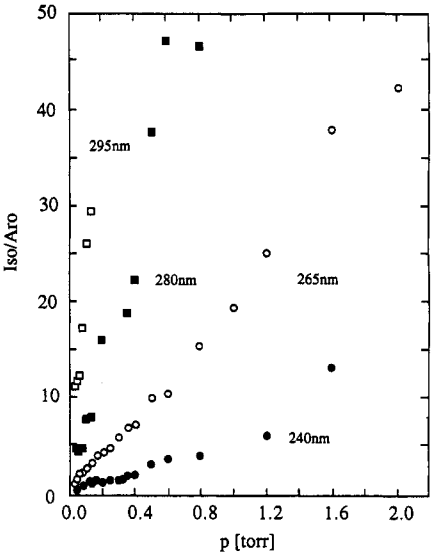

Figure 3. Ratio of positional isomerization products to structural isomerization products in the self-quenching photolysis of 7-Et-CHT.

This behavior is consistent with rapid establishment of equilibrium among the positional isomers before they are collisionally stabilized. Data at other wavelengths are similar except that the pressure-dependent region extends to successively higher pressures with increasing energy of photolysis radiation. Table I shows that as the excitation wavelength decreases at constant pressure, the yield of structural isomerization products increases. This is consistent with the formation of a photoactivated intermediate having the expected trend of decreasing isomerization lifetime with increasing energy.

The ratio of positional isomerization products to structural isomerization products in Figure 3, increasing with increasing pressure at fixed wavelength and increasing with increasing wavelength at fixed pressure, is consistent with a shorter lifetime for positional isomerization than for structural isomerization.

To further examine the proposition that the equilibrium of positional isomers is attained before structural isomerization, theoretical calculations were done as described in the following sections, for all positional and structural isomerization reactions. Since k_∞ for each positional isomerization reaction was not available, it was assumed that positional isomerization occurs via the same 1,5-hydrogen-transfer reaction as 7-Me-CHT. Furthermore, in general, the activation energies for 1,5-hydrogen transfer are not sensitive to changes in the substituents of the basic cisoid structure of the molecule.[19] The same k_∞ as that of 7-Me-CHT was adopted.

$$k_\infty = 10^{12.80} \exp(-33.25\ (\text{kcal/mol})/RT) \qquad (1)$$

To meet the above k_∞ value, activated complex frequencies were obtained by multiplying the activated molecule frequencies in the Appendix by 0.9705 after omitting the 223-cm^{-1} vibrational frequency. Quantum yields were calculated from the master

(19) Glass, D. S.; Boikess, R. S.; Winstein, S. *Tetrahedron Lett.* **1966**, *10*, 999.

TABLE II: Calculated Total Quantum Yield of Positional and Structural Isomerization Reaction of 7-Et-CHT[a]

	quantum yield			
p, Torr	240 nm, $\langle\Delta E\rangle$ = 3.75 kcal/mol	265 nm, $\langle\Delta E\rangle$ = 1.9 kcal/mol	280 nm, $\langle\Delta E\rangle$ = 1.25 kcal/mol	295 nm, $\langle\Delta E\rangle$ = 0.95 kcal/mol
0.4	1.0	1.0	1.0	1.0
0.8	1.0	1.0	1.0	0.9995
1.2	0.9996	0.9992	0.9988	0.9957
1.6	0.9985	0.9968	0.9949	0.9852
2.0	0.9961	0.9916	0.9872	0.9681
4.0	0.9618	0.928	0.9025	0.8349
8.0	0.8376	0.7514	0.7012	0.6025
16.0	0.6207	0.5123	0.46	0.3733
20.0	0.5446	0.4391	0.3904	0.3125

[a] The pressure range in this work was 0–2 Torr.

equation by using $\langle\Delta E\rangle$ values obtained in this work for the structural isomerization. The results of the quantum yield calculation for the all isomerization reaction are in Table II. It is shown that, in our experimental pressure ranges, i.e., 0–2 Torr, the quantum yields are almost one at each wavelength and the assumption is acceptable.

Quantum Yields. With constant pressure and temperature during reaction and by use of Lambert–Beer's law, the product quantum yield at pressure p is

$$\Phi = \frac{(pV/RT)(df/dt)}{I_0(1 - 10^{-\epsilon pl/RT})} \tag{2}$$

where V is the reactor volume, R the gas constant, T the temperature, f the fraction of products, I_0 the incident light intensity, ϵ the extinction coefficient, and l the length of the reactor. Since the quantum yield approaches one as the pressure approaches zero,[3] it is possible to remove I_0 and V/RT from eq 2.

$$\Phi = \frac{\Phi}{\Phi|_{p\to 0}} = \frac{p(df/dt)/(1 - 10^{-\epsilon pl/RT})}{p(df/dt)/(1 - 10^{-\epsilon pl/RT})|_{p\to 0}} \tag{3}$$

When the total probability of being deactivated is S and the total probability of isomerization is D (=1 − S), the quantum yield can also be expressed as

$$\Phi = D/(S + D) \tag{4}$$

From the above equation, D/S is obtained as

$$D/S = \Phi/(1 - \Phi) \tag{5}$$

Therefore, experimentally, Φ and D/S can be obtained by measuring the change of the fraction of products, i.e., sum of the percentages of structural isomerization products in this experiment, with time at each pressure.

First, with the structural isomerization product analysis data, df/dt at each pressure was obtained. The change of percentage concentration of products is linear with time within 5% conversion range. Then, since the incident light intensity, I_0, and the light intensity exiting from the reactor, I, has the following relationship

$$\log (I/I_0) = -\epsilon pl/RT \tag{6}$$

with the slope of the graph of −log (I/I_0) vs. p at each wavelength,

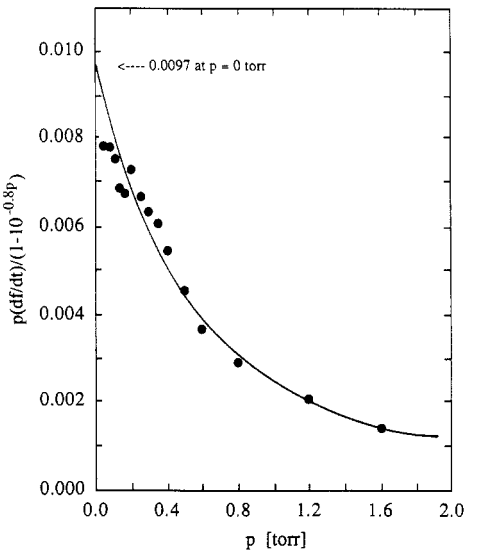

Figure 4. Steady-state values of $(df/dt)/(1 - 10^{-0.8p})$ in the photolysis at 240 nm.

$\epsilon l/RT$ was obtained for the corresponding light source–monochromator or filter combination. Graphs of $p(df/dt)/(1 - 10^{-\epsilon pl/RT})$ vs. p were drawn with these values of $\epsilon l/RT$ and df/dt. The value at zero pressure was obtained by extrapolating a smooth curve through the data points to zero pressure. These limiting values at each wavelength could also be obtained in the following way which gave the same results. By l'Hospital's rule

$$\lim_{p\to 0} \frac{p(df/dt)}{1 - 10^{-\epsilon pl/RT}} = \frac{1}{2.303(\epsilon l/RT)} \lim_{p\to 0} df/dt \tag{7}$$

Therefore, by extrapolating the graph of df/dt vs. p to p = 0, we could obtain the value of $p(df/dt)/(1 - 10^{-\epsilon pl/RT})$ at zero pressure. Figure 4 shows extrapolation of the 240-nm data. Extrapolations at other wavelengths were similar. With these data, the quantum yield, Φ, and D/S at each wavelength were obtained.

To investigate uncertainties in the extrapolation to zero pressure, three other methods were also used. First, quantum yields calculated from eq 3 were forced to agree with the Stern–Volmer equation 8, using Stern–Volmer constants $a(M)$, reported in ref

$$1/\Phi = 1 + a(M)p \tag{8}$$

3 by adjusting $p(df/dt)/(1 - 10^{-\epsilon pl/RT})|_{p=0}$. Second, least-squares orthogonal polynomial data fitting was done using a program supplied by the University of Minnesota Computer Center. The polynomial fits to the experimental data were then extrapolated to p = 0 without adjusting the coefficients. Finally, the lowest pressure data point at each wavelength was chosen as a lower limit estimate of $p(df/dt)/(1 - 10^{-\epsilon pl/RT})|_{p=0}$. The last procedure is useful insofar as it sets a lower bound on this quantity and, therefore, also on $\langle\Delta E\rangle$. The intercepts obtained by these three methods are listed in Table III.

Stern–Volmer curves at each wavelength are in Figure 5. The solid lines are linear fits which were used to adjust the scale of $1/\Phi$ so that agreement of $a(M)$ with published values could be obtained, as outlined in the previous paragraph. The data, how-

TABLE III: Values of $p(df/dt)/(1 - 10^{-\epsilon pl/RT})|_{p=0}$ Obtained by Three Different Methods and Their Effect on $\langle\Delta E\rangle$

	from Stern–Volmer constants				from least-squares orthogonal polynomial data fitting				from the lowest pressure data points			
λ, nm	intercept value at p = 0	$a(M)$, Torr^{-1}	$\langle\Delta E\rangle$, kcal/mol model I	$\langle\Delta E\rangle$, kcal/mol model II	intercept value at p = 0	$a(M)$, Torr^{-1}	$\langle\Delta E\rangle$, kcal/mol model I	$\langle\Delta E\rangle$, kcal/mol model II	intercept value at p = 0	$a(M)$, Torr^{-1}	$\langle\Delta E\rangle$, kcal/mol model I	$\langle\Delta E\rangle$, kcal/mol model II
240	0.0097	3.2[a]	3.75 ± 1.25	3.35 ± 1.15	0.0089	2.7	3.0 ± 1.0	2.8 ± 1.0	0.0079	2.27	2.0 ± 0.5	1.9 ± 0.5
265	6.2	11.3	2.45 ± 0.75	2.15 ± 0.65	3.8	5.9	0.85 ± 0.15	0.8 ± 0.15	3.7	5.84	0.78 ± 0.12	0.73 ± 0.13
280	0.019	15.0[b]	1.1 ± 0.3	1.05 ± 0.25	0.017	13.3	0.75 ± 0.15	0.73 ± 0.12	0.013	9.44	0.6 ± 0.1	0.56 ± 0.1
295	0.013	40.0[b]	1.05 ± 0.25	1.0 ± 0.3	0.0079	24.2	0.55 ± 0.15	0.55 ± 0.15	0.007	17.54	0.48 ± 0.12	0.44 ± 0.1

[a] This value was interpolated form the data at 237.8 and 249.2 nm in ref 3. [b] These values were extrapolated from the data in ref 3 assuming $a(M)$ of 7-Et-CHT changes in the same way as that of 7-Me-CHT.

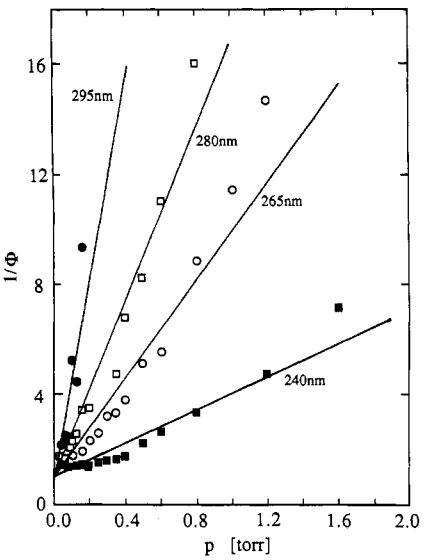

Figure 5. Stern–Volmer curves of self-quenching photolysis of 7-Et-CHT.

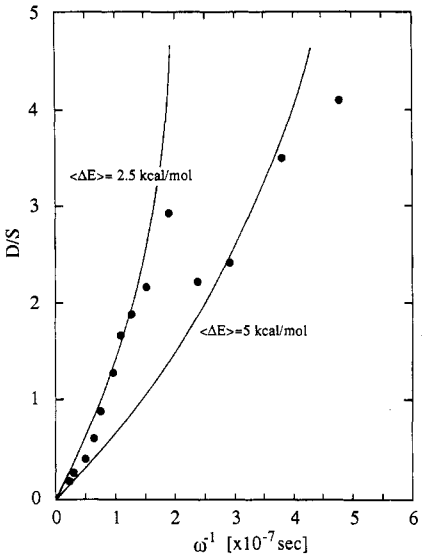

Figure 6. Data fitting of experimental values to theoretical values of D/S with $\langle\Delta E\rangle$ as the parameter at 240 nm (model I).

ever, show curvature in the low-pressure region, indicative of multistep collisional deactivation. Although deactivation step sizes could have been obtained from RRKM analysis of Stern–Volmer plots, an alternative treatment in which D/S was plotted vs. ω^{-1}, the reciprocal of the collision frequency, which expands the low-pressure region and permits more sensitive determination of step size was used. Figures 6–9 show the data plotted this way. Experimental measurements were not done at lower pressures since decomposition of the structural isomers would have become significant enough to cause D/S to be appreciably underestimated.

Theoretical Calculations. The multistep deactivation model with uniform deactivation step size was applied for the theoretical calculation of Φ and D/S. The quantum yield, Φ, was calculated from the master equation in matrix formulation

$$\Phi = (1/\omega)\sum_i(\mathbf{k}(\mathbf{I} - \mathbf{p} + \mathbf{k}/\omega)^{-1}\mathbf{f})_i \qquad (9)$$

where i is the ith energy level, $\mathbf{k}$ is a main diagonal matrix with decomposition rate constants k_i as its elements, $\mathbf{p}$ is a transition probability matrix with elements p_{ij}, and $\mathbf{f}$ is a column matrix of fractional rates of input with elements f_i. Since the bandwidths of incident light are relatively narrow, a δ function was used for f_i, the fraction entering the ith energy level when excited. Negligible error was introduced by this simplification. It has been shown that weak colliders, small molecules which remove small amounts of energy per collision, tend to show the exponential type of distribution while large molecules exhibit stepladder behavior.[20]

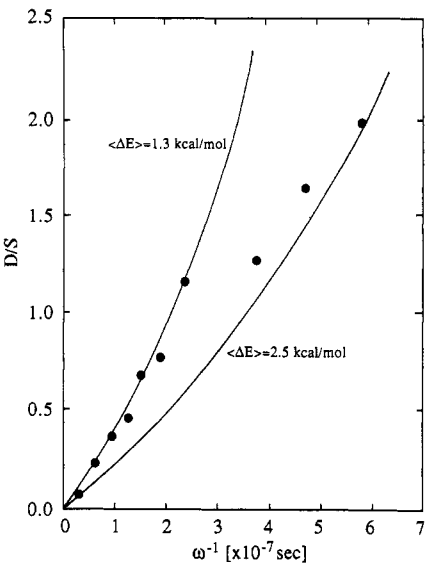

Figure 7. Data fitting of experimental values to theoretical values of D/S with $\langle\Delta E\rangle$ as the parameter at 265 nm (model I).

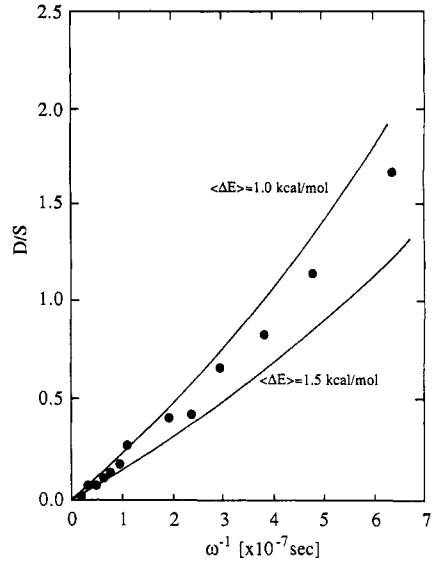

Figure 8. Data fitting of experimental values to theoretical values of D/S with $\langle\Delta E\rangle$ as the parameter at 280 nm (model I).

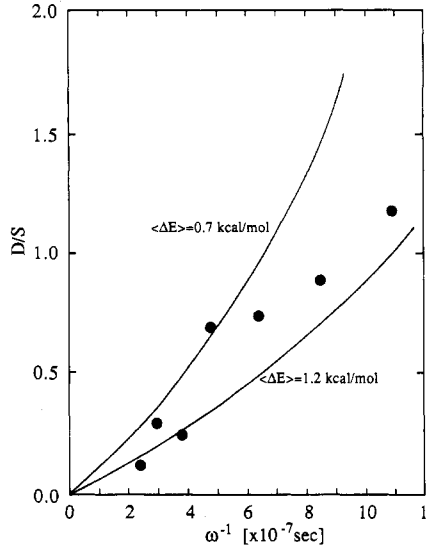

Figure 9. Data fitting of experimental values to theoretical values of D/S with $\langle\Delta E\rangle$ as the parameter at 295 nm (model I).

TABLE IV: Energy-Dependent Rate Constant, $k(E)$, Calculated from RRKM Theory

energy of active molecule, E^*, kcal/mol	$k(E)$, s^{-1}	energy of active molecule, E^*, kcal/mol	$k(E)$, s^{-1}
52.64	1.96×10^{-2}	102.64	1.85×10^{5}
62.64	3.68	107.64	3.82×10^{5}
72.64	2.31×10^{2}	112.64	7.39×10^{5}
82.64	4.01×10^{3}	117.64	1.35×10^{6}
92.64	3.41×10^{4}	122.64	2.36×10^{6}
97.64	8.31×10^{4}		

In this work with a large molecule, 7-Et-CHT, the stepladder model was used for p_{ij}, the collisional transition probabilities from jth level to ith level.

Microcanonical decomposition rate constants, $k(E)$, for each energy level, were computed by using RRKM theory of unimolecular reactions

$$k(E) = L^{\ddagger}\frac{Q_1^{\dagger}}{Q_1}\frac{\sum_{E_0}^{E} P(E - E_0)}{hN(E)} \qquad (10)$$

where $L^{\ddagger}$ is the number of the geometrically equivalent reaction paths, Q_1 and $Q_1^{\dagger}$ are partition functions for the adiabatic rotations of the reactant and the activated complex, h is Planck's constant, $\sum P$ is the sum of quantum states of transition state, and N is the density of quantum states of active molecules. For the sum and the density of quantum states, counting of vibrational states was done in the direct counting method with the Beyer–Swinehart algorithm[21,22] with a grain size of 0.01 kcal/mol. The harmonic oscillator models for the activated molecules in the Appendix were obtained from ref 5. For the activated complex, one 420-cm^{-1} vibration was taken as the reaction coordinate. All other frequencies were multiplied by 0.993 in order to normalize to experimental values of $k(E)$ determined by direct detection by Hippler et al.[4] The average total energy excited molecule was calculated as the sum of the thermal energy and the photon energy. Thermal energy at 300 K was about 3.6 kcal/mol.[6] So, after light absorption, the energies of the excited molecules were 122.6 kcal/mol at 240 nm, 111.4 kcal/mol at 265 nm, 105.6 kcal/mol at 280 nm, and 100.4 kcal/mol at 295 nm. Calculated $k(E)$ values are in Table IV.

The collision frequency, ω, is expressed as the multiplication of collision number, Z, and pressure, p

$$\omega = Zp = \pi d^2(16RT/\pi M)^{1/2}(L/RT)p \qquad (11)$$

where d is the collision diameter, R the gas constant, T the temperature, M the molecular weight, and L Avogadro's number. Molecular parameters for the calculation of collision frequency are in the Appendix. Collision diameter was calculated by multiplying the Lennard-Jones constant, σ, by the square root of the reduced collision integral, $\Omega^{*(2,2)}$. Two sets of molecular parameters, model I from ref 6 and model II from ref 9, were available and studied the effect of the parameter differences. Calculated Z's are 2.62×10^7 with model I and 2.75×10^7 [$Torr^{-1}$ s^{-1}] with model II. In case of using internal standard, collision number with internal standard, Z_{AI}, is

$$Z_{AI} = \pi d_{AI}^2(8RT/\pi\mu_{AI})^{1/2}(L/RT) \qquad (12)$$

where subscript A stands for 7-Et-CHT and I for internal standard. The following Lennard-Jones parameters were used:

$$\sigma_{AI} = \sigma_A + \sigma_I \quad \text{and} \quad \epsilon_{AI} = (\epsilon_A\epsilon_I)^{1/2} \qquad (13)$$

Then, when y_I is the fraction of internal standard, the total collision number becomes

$$Z = Z_{AA}(1 - y_I) + Z_{AI}y_I \qquad (14)$$

Calculated Z_{AI}'s are 2.62×10^7 with model I and 2.63×10^7 [$Torr^{-1}$ s^{-1}] with model II.

D/S was calculated from eq 5 with Φ values obtained from eq 9, and $\langle\Delta E\rangle$ was obtained by fitting the theoretical calculations of D/S to the experimental results of D/S using $\langle\Delta E\rangle$ as an adjustable parameter. Here, since positional isomers have similar structure it was assumed that $\langle\Delta E\rangle$'s for positional isomers are the same.

Discussion

The aromatic reaction products formed by isomerization of activated ethylcycloheptatrienes have sufficient energy to dissociate. If they do so to an appreciable extent, D/S would be underestimate and $\langle\Delta E\rangle$ overestimated. That this is not the case in this work can be shown as follows. Assuming that the isomerization is exothermic by 31.6 kcal/mol, which is the enthalpy change for cycloheptatriene → toluene,[23] the aromatics will initially be activated to energies from 131.6 kcal/mol (290-nm excitation) to 154.6 kcal/mol (240-nm excitation). The dissociation of toluene to benzyl and H requires 86.3 kcal/mol,[24] and the activation energy for decomposition of ethylbenzene is greater than 81.3 kcal/mol.[25] Using a conservative estimate of 80 kcal/mol for the threshold energy for dissociation of propyl- and methylethylbenzenes, RRKM theory was used to make estimates of $k(E)$. With the Marcus–Rice[26,27] expression for sums and densities of states, $k(E)$ is estimated to be 10^2 s^{-1} at 290 nm and 2×10^3 s^{-1} at 240 nm. A similar calculation for Et-CHT → aromatics at 248 nm gave $k(E) = 3.2 \times 10^6$ s^{-1}, which may be compared with the experimental value, 1.5×10^6 s^{-1}.[25] We conclude that the lifetime for decomposition of the aromatics is approximately 10^3 longer than the lifetime for isomerization of Et-CHT. Since the maximum value of D/S attained here is about 4 (Figure 8), secondary decomposition of the aromatics must be less than 1% and can be safely dismissed as a possible influence on $\langle\Delta E\rangle$.

Figures 6–9 show D/S vs. ω^{-1} where the quantum yields for use in eq 5 were obtained by requiring $\lim_{p\to 0} p(df/dt)/(1 - 10^{-\epsilon pl/RT}) = 1/(2.303\epsilon l/RT)\lim_{p\to 0} df/dt$ from extrapolation of $p(df/dt)/(1 - 10^{-\epsilon pl/RT})$ and df/dt to $p = 0$. The two solid lines in each figure are the theoretical calculations from model I that bound the experimental data. Values of $\langle\Delta E\rangle$ were obtained by averaging the bounding values of $\langle\Delta E\rangle$. From Figures 6–9 with model I, $\langle\Delta E\rangle$ was 3.75 ± 1.25 kcal/mol at 240 nm, 1.9 ± 0.6 kcal/mol at 265 nm, 1.25 ± 0.25 kcal/mol at 280 nm, and 0.95 ± 0.25 kcal/mol at 295 nm. The same data fittings were done with model II, and $\langle\Delta E\rangle$ was 3.35 ± 1.15 kcal/mol at 240 nm, 1.75 ± 0.55 kcal/mol at 265 nm, 1.1 ± 0.3 kcal/mol at 280 nm, and 0.9 ± 0.2 kcal/mol at 295 nm. All these calculations were done on the University of Minnesota Cyber 170-825 computer.

These $\langle\Delta E\rangle$ values are plotted as a function of E^* in Figure 10, which also shows $\langle\Delta E\rangle$ obtained from direct detection by time-resolved UV absorption following pulsed laser excitation at 248 nm[6] and a revised $\langle\Delta E\rangle$[6] from the previous indirect study.[3] The first investigation of 7-Et-CHT, by Troe and Wieters,[3] was done by steady-state photoisomerization, monitoring light absorption to follow disappearance of the parent, whereas in this work, reaction products were determined by gas chromatography. The absolute values of $\langle\Delta E\rangle$ from three different experimental methods are in excellent agreement in that they all fall smoothly on the same curve. The accord between the indirect studies comes from the use of identical values of $k(E)$ and collision frequencies and gives evidence for the compatibility of the data. The agreement with the directly measured $\langle\Delta E\rangle$, which is independent of $k(E)$, although it depends upon ω, is a validation of the indirect method. Indirect methods for investigating energy transfer are acceptable provided the chemistry is understood, and accurate

(20) Forst, W. *Theory of Unimolecular Reactions*, 1st ed.; Academic: New York, 1973.
(21) Beyer, T.; Swinehart, D. F. *Commun. ACM* **1973**, *16*, 379.
(22) Stein, S. E.; Rabinobitch, B. S. *J. Chem. Phys.* **1973**, *58*, 2438.
(23) Atkinson, R.; Thrush, B. A. *Proc. R. Soc. London, A* **1970**, *316*, 143.
(24) Asholz, D. C.; Durant, J.; Troe, J. *Symp. (Int.) Combust. [Proc.], 18th* **1981**, 885.
(25) Brouwer, L.; Muller-Markgraf, W.; Troe, J. *Ber. Bunsenges. Phys. Chem.* **1983**, *87*, 1031.
(26) Marcus, R. A.; Rice, O. K. *J. Phys. Colloid Chem.* **1951**, *55*, 894.
(27) Marcus, R. A. *J. Chem. Phys.* **1952**, *21*, 359.

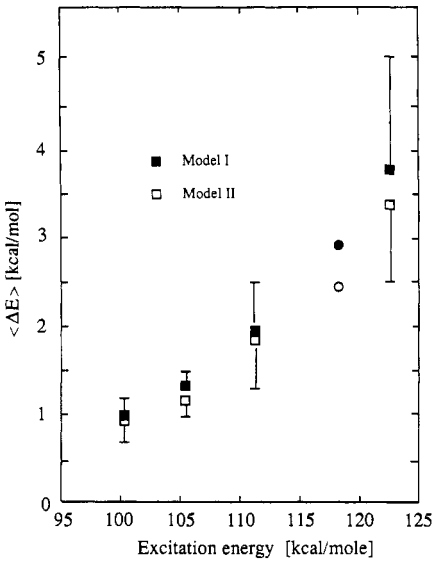

Figure 10. $\langle\Delta E\rangle$ change with the excitation energy of 7-Et-CHT at each wavelength. Range notations are for model I. Model II has almost the same range. ● denotes the value from the direct measurement of ref 6. O denotes the value, from the steady-state photolysis in ref 9, down revised after adopting new $k(E)$.

values of $k(E)$ and ω are available for fitting the data.

The energy dependence of $\langle\Delta E\rangle$ shown in Figure 10 appears visually to be nonlinear with monotone upward curvature. However, a linear relationship over this energy range cannot be ruled out. A straight line passes through the data when the error limits are taken into account. In fact, the plotted data points at 100, 106, 111, and 119 kcal/mol all lie very close to a straight line, although a curve may be a slightly better fit. A straight line through these data would extrapolate a positive intercept in the vicinity of 90 kcal/mol. Since $\langle\Delta E\rangle$ cannot be zero at this energy, it must be concluded that if the relationship is linear between 100 and 123 kcal/mol, the slope (curvature) must become smaller (shallower) below 100 kcal/mol.

The results of an investigation of the effect of different zero-pressure extrapolations on the values of $\langle\Delta E\rangle$ are summarized in Table III. When literature values of Stern–Volmer constants are used, $\langle\Delta E\rangle$ at 240 nm is in excellent agreement with $\langle\Delta E\rangle$ from Figure 6, and $\langle\Delta E\rangle$'s at 265, 280, and 295 nm are within experimental error of $\langle\Delta E\rangle$'s from Figures 7–9, respectively. At 280 and 295 nm, Stern–Volmer constants were estimated by assuming that they had the same energy dependence as 7-Me-CHT, for which $a(M)$ values have been reported over the same energy range. Using a polynominal fit to the data gives smaller intercepts and smaller $\langle\Delta E\rangle$'s at each wavelength, and the lower bound to the intercepts obtained from the lowest pressure data point gives the smallest value of $\langle\Delta E\rangle$, as expected. The $\langle\Delta E\rangle$'s from the last procedure must be somewhat smaller than the true value. It is significant that in all cases, the $\langle\Delta E\rangle$'s decreased with decreasing excitation energy.

The energy dependence of $\langle\Delta E\rangle$ reported here is clearly at variance with the work of Hippler, Troe, and Wendelken,[6] who were unable to find any energy dependence of $\langle\Delta E\rangle$ for Et-CHT by the UV absorption method. The results in Figure 10 and Table III cannot be reconciled with an energy independent $\langle\Delta E\rangle$ if the stepladder model is a sufficiently accurate representation of the collisional transition probability. The stepladder model has generally been found to be adequate for polyatomic molecules.[20]

A difference between the two experimental methods is that, in UV absorption, $\langle\Delta E\rangle$ can be followed over the entire energy range from initial excitation energy to the thermal equilibrium energy while product quantum yield measurements must give $\langle\Delta E\rangle$ values for energies above the reaction threshold. In fact, product measurements will give $\langle\Delta E\rangle$'s that are weighted toward the initial excitation energy, since $k(E)$ is a strong function of energy while ω is not. In spite of this difference the absolute values of $\langle\Delta E\rangle$ from the present work, which are valid for some energy range near the excitation energy, are in excellent agreement with the value from UV absorption.

A further difference is that to obtain $\langle\Delta E\rangle$ from time-resolved UV absorption the extinction coefficient must be known as a function of energy. This is usually calibrated via independent experiments. The reason(s) for the difference between the energy dependence of $\langle\Delta E\rangle$ from direct and indirect experiments must lie in the differences between the two methods of obtaining and treating the data. It would be speculative to attempt to identify the reasons at present. The indirect method, as used here, should give accurate measurements of $\langle\Delta E\rangle$ provided the chemistry is understood, accurate values of $k(E)$ are available, and a good collisional transition probability model is used. For 7-Et-CHT the first two criteria appear to be met. The third one will be examined in the near future.

Appendix

Activated molecule frequencies (in cm^{-1}) of 7-Et-CHT:[28] 3066, 3039, 3026 (4), 3000 (4), 2966, 2838, 1609 (2), 1535, 1433, 1415 (6), 1393, 1298, 1235, 1218 (2), 1192, 1049, 1020, 1000 (2), 994, 973, 952, 920, 908, 876, 792, 743, 712, 657, 650, 600, 588, 428, 421, 420 (4), 405, 355, 291, 223.

Two free internal rotors: $B_1 = 5.621$ cm^{-1}, $\sigma_1 = 3$; $B_2 = 0.992$ cm^{-1}, $\sigma_2 = 1$. B_i = effective rotational constant = $h/(8\pi^2 c I_i)$, where h is Planck's constant, c the velocity of light, and I the moment of inertia. σ_i = symmetry number.

Lennard-Jones collision parameters from the boiling point and critical data correlation of 7-Et-CHT:

Model I.[6] $T_b = 417$ K (obtained by extrapolating the vapor pressure data of ref 14 and 29), $T_c = 619$ K, $p_c = 32.95$ atm (by Lydersen's method as modified by Fishtine[30]), $\omega = 0.335$, $\sigma = 6.52$ Å, $\epsilon/k = 406$ K, $\Omega^{*(2,2)} = 1.8682$ at 298 K; from $T_b/T_c = 0.567 \pm \sum\Delta_T - (\sum\Delta_T)^2$, $p_c = M/(\sum\Delta_p + 0.34)^2$; Δ quantities were evaluated by summing contributions for various atoms and groups of atoms in Table 2-1 (Lydersen's method); $\omega = (3/7)[T_b/(T_c - T_b)](\log p_c) - 1$ (ref 31), $\sigma = (2.3454 + 0.2972\omega)(T_c/p_c)^{1/3}$, $\epsilon/k = (0.8082 - 0.4504\omega)T_c$ (ref 10), $\Omega^{*(2,2)} = 1.16145/(T^{*0.14874}) + 0.52487/\exp(0.7732T^*) + 2.16178/\exp(2.4379T^*)$ where $T^* = T/(\epsilon/k)$ (ref 32).

Model II.[3,17] $T_b = 443$ K (estimated from the corresponding aromatic isomers), $T_c = 660$ K, $p_c = 32.95$ atm, $Z_c = 0.254$ (Lydersen's method), $\sigma = 7.225$ Å, $\epsilon/k = 310$ K, $\Omega^{*(2,2)} = 1.5967$ at 298 K; from $V_c = 40 + \Sigma\Delta_v$, $Z_c = p_c V_c/RT_c$ (Lydersen's method); $\sigma = 0.1866 V_c^{1/3} Z_c^{-6/5}$, $\epsilon/k = 65.3 T_c Z_c^{18/5}$ (Stiel–Thodos method) (ref 32), $\Omega^{*(2,2)} = [0.636 + 0.567 \log T^*]^{-1}$ (ref 33).

Lennard-Jones collision parameters of internal standard hexane:[32] $\sigma_1 = 5.949$ Å, $\epsilon_1/k = 399.3$ K, $\Omega_{AI}{}^{*(2,2)} = 1.867$ (model I) and 1.68 (model II) at 298 K.

Registry No. 7-Et-CHT, 17634-51-4; 1-Et-CHT, 16731-87-6; 2-Et-CHT, 17635-00-6; 3-Et-CHT, 17634-50-3; *o*-MeC_6H_4Et, 611-14-3; *m*-MeC_6H_4Et, 620-14-4; *p*-MeC_6H_4Et, 622-96-8; *n*-PrPh, 103-65-1.

(28) Benson, S. W. *Thermochemical Kinetics*, 2nd ed.; Wiley: New York, 1976.
(29) Miyano, S.; Hashimoto, H. *Bull. Chem. Soc. Jpn.* **1973**, *46*, 3257.
(30) Fishtine, S. H. *Z. Phys. Chem.* **1980**, *123*, 39.
(31) Mourits, F. M.; Rummens, F. H. A. *Can. J. Chem.* **1977**, *55*, 3007.
(32) Reid, R. C.; Prausnitz, J. M.; Sherwood, T. K. *The Properties of Gases and Liquids*, 3rd ed.; McGraw-Hill: New York, 1977; pp 12–19, 395–399.
(33) Troe, J. *J. Chem. Phys.* **1977**, *66*, 4758.